Journal of Zhejiang University-SCIENCE A (Applied Physics & Engineering)
ISSN 1673-565X (Print); ISSN 1862-1775 (Online)
www.zju.edu.cn/jzus; www.springerlink.com
E-mail: jzus@zju.edu.cn

Dimensionless study on outlet flow characteristics of an air-driven booster*

Yan SHI, Mao-lin CAI

(*School of Automation Science and Electrical Engineering, Beihang University, Beijing 100191, China*)

E-mail: yesoyou@gmail.com; caimaolin@gmail.com

Received July 4, 2011; Revision accepted Feb. 28, 2012; Crosschecked May 16, 2012

Abstract: Air-driven boosters are widely used to obtain high-pressure gas. Through analysis of the boosting process of an air-driven booster, the basic mathematical model of working processes can be set up. By selecting the appropriate reference values, the basic mathematical model is transformed to a dimensionless expression. Using MATLAB/Simulink for simulation and studying the booster experimentally, the dimensionless outlet flow characteristics of the booster were obtained and the simulation results agree well with the experimental results. Through analysis, it can be seen that the dimensionless outlet flow of the booster is mainly determined by the dimensionless input pressure of the driving chamber, the dimensionless outlet condition pressure of the booster and the dimensionless area of the piston in the driving chamber. The dimensionless average outlet flow becomes larger with an increasing dimensionless input pressure of the driving chamber, but it becomes smaller with an increase in the dimensionless outlet condition pressure of the booster. Especially when the dimensionless outlet condition pressure is approximately 1.4, the dimensionless average outlet flow reaches zero. With an increase in the dimensionless area of the piston in the driving chamber, the dimensionless average outlet flow increases and peaks at approximately 1.89, and after this peak, it starts to decrease. This research can be referred to in the design of air-driven boosters.

Key words: Air-driven booster, Outlet flow, Pneumatic system, Compressed air
doi:10.1631/jzus.A1100176 **Document code:** A **CLC number:** TH138

1 Introduction

Pressure-boosting technologies have been ultilized in many fields, such as the pneumatic system, vacuum machinery, natural gas industry, and cryogenics engineering (Cheng *et al*., 2003; Hernández and Jorge, 2005; Chapman *et al*., 2008; Cho *et al*., 2009; Ge and Tassou, 2011). Compared with the multistage high-pressure compressor, air-driven boosters have the advantages of having a more compact structure, a smaller size, fewer moving parts and seals, lighter weight, and no external power, and they are used widely in local pressure-boosting occasions, where there is a require for a small amount of higher pressure air (Li *et al*., 2007; SMC (China) Co., Ltd, 2008). For example, the high-pressure injection of natural gas directly into the combustion chamber of a combustion ignition engine is considered to be the best method to achieve the highest extraction of energy from this fuel (Reed Business Information (Cahners), 2003). Moreover, with the popularization and development of energy-saving technologies of the pneumatic system, air-driven pressure boosters are usually used for reducing outlet pressure of air compressors and cutting down energy consumption of air compressors (Shi *et al*., 2010). However, the booster has drawbacks. For example, a booster has a short lifespan, and its outlet flow is small; when boosting-rate is high, these shortages become more distinct. Additionally, its energy efficiency is not high, which also restricts its application and popularization (Takeuchi *et al*., 1995; Shi *et al*., 2010). To

* Project supported by the Innovation Foundation of Beihang University for PhD Graduates, China

develop a booster with better performance, further research on its outlet flow characteristics is essential. In this paper, a dimensionless mathematical model of an air-driven booster is presented, and the simulation results are shown and discussed. Lastly, the dimensionless mathematical model was verified experimentally, and errors in the simulation results and the experimental results were analyzed.

2 Principles of an air-driven booster

As illustrated in Fig. 1, a typical air-driven booster consists of a piston, a regulator, two boosting chambers, two driving chambers, four check valves, and a reversing valve (Shi *et al*., 2010a; 2010b).

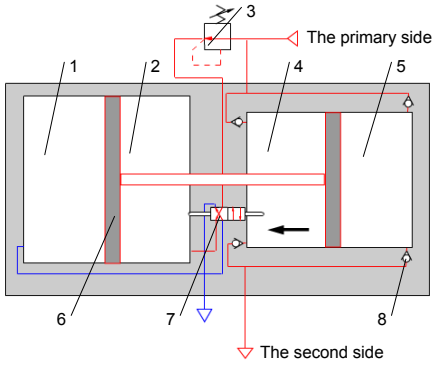

1: driving chamber A; 2: driving chamber B; 3: regulator; 4: boosting chamber A; 5: boosting chamber B; 6: piston; 7: reversing valve; 8: check valve

Fig. 1 Structure of an air-driven booster

The working process of the air-driven booster can be found in our previous study (Shi and Cai, 2011). The higher pressure compressed air is discharged continuously by repeating the working process, which can be seen in the following Figs. 3, 4 and 6.

In this study, we define the pressure of the higher-pressure air delivered from the boosting chamber as the outlet pressure, P_o, and the pressure of the secondary side as the outlet condition pressure, $P_{o\text{-condition}}$. It is obviously that the outlet pressure of the booster is not equal to the outlet condition pressure.

3 Basic mathematical model

To facilitate the study, the following assumptions are made:

1. There is no leakage between the four chambers, the area of the piston rod end is so small that can be neglected, and the effective areas of all charge and discharge ports are the same.

2. The compressed air of the system follows the ideal gas law.

3. The compressed air flow of the booster is 1D state-steady flow, which is the same as the air flow through the nozzle contraction.

4. The temperature of the compressed air is equivalent to the atmospheric temperature.

3.1 Energy equation

Each chamber was considered as one control unit, and the whole booster was considered as the coordinate system. In respect that there is no leakage between the chambers, all of the chambers do not exhaust and charge air simultaneously. Therefore, the energy equation for the intake and exhaust sides of every chamber can be obtained:

$$C_v m\frac{\mathrm{d}\theta}{\mathrm{d}t}=(S\cdot h+C_v\cdot G)(\theta_a-\theta)+RG\theta_a-PAu, \quad (1)$$

$$C_v m\frac{\mathrm{d}\theta}{\mathrm{d}t}=S\cdot h(\theta_a-\theta)+RG\theta-PAu, \quad (2)$$

where C_v is the specific heat at constant volume, m is the mass of the compressed air, θ is the temperature, θ_a is the atmosphere temperature, t is the time, S is the heat transfer area, h is the heat transfer coefficient, R is the gas constant, G is the mass flow of the compressed air, P is the pressure, A is the area of piston, and u is the velocity of piston.

3.2 Equation of continuity

According to the law of mass conservation, the air mass can be given as

$$\frac{\mathrm{d}m}{\mathrm{d}t}=G. \quad (3)$$

3.3 Flow equation

Based on the ratio P_L/P_U, the flow equation for the flow through a restriction can be given as

$$G=\begin{cases}\dfrac{A_e P_U B}{\sqrt{\theta_U}}\varphi(P_U,P_L), & \dfrac{P_L}{P_U}>0.528,\\ \dfrac{A_e P_U D}{\sqrt{\theta_U}}, & \dfrac{P_L}{P_U}\le 0.528,\end{cases} \quad (4)$$

where

$$\varphi(P_{\mathrm{U}},P_{\mathrm{L}})=\left[\left(\frac{P_{\mathrm{L}}}{P_{\mathrm{U}}}\right)^{\frac{2}{\kappa}}-\left(\frac{P_{\mathrm{L}}}{P_{\mathrm{U}}}\right)^{\frac{\kappa+1}{\kappa}}\right], \tag{5}$$

$$B=\sqrt{\frac{2\kappa}{R(\kappa-1)}}, \tag{6}$$

$$D=\left(\frac{2}{\kappa+1}\right)^{\frac{1}{\kappa-1}}\sqrt{\frac{2\kappa}{R(\kappa+1)}}. \tag{7}$$

where P_L and P_{U} is the pressure of downstream side and upstream side, respectively, A_{e} is the effective area of intake and exhaust ports, θ_{U} is the temperature of upstream side, and κ is the specific heat ratio.

The average outlet flow of the booster is the average value of one period.

$$\overline{G}=\frac{m}{t}. \tag{8}$$

3.4 Motion equation

The piston velocity can be given from Newton's second law of motion. In this study, the friction force is considered to be the sum of the viscous friction and the Coulomb friction. The viscous friction force is reckoned to be a linear function of the piston velocity. The forces on the piston are illustrated in Fig. 2.

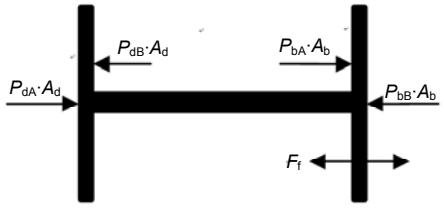

P_{dA} and P_{dB} is the pressure of the driving chamber A and chamber B, respectively; P_{bA} and P_{bB} is the pressure of the boosting chamber A and chamber B, respectively; A_d and A_b is the piston area of the driving chamber and boosting chamber, respectively

Fig. 2 The forces on the piston of the booster

The right side is figured to be the positive direction of the vector. The piston motion equation can be obtained as follows:

$$\frac{\mathrm{d}^2x}{\mathrm{d}t^2}=\begin{cases}(P_{\mathrm{dA}}A_{\mathrm{d}}-P_{\mathrm{dB}}A_{\mathrm{d}}+P_{\mathrm{bA}}A_{\mathrm{b}}-P_{\mathrm{bB}}A_{\mathrm{b}}-F_{\mathrm{f}})/M, \\ \quad x\neq 0,L, \\ 0,\ x=0,L,\end{cases} \tag{9}$$

where

$$F_{\mathrm{f}}=\begin{cases}F_{\mathrm{s}}, & u=0, \\ F_{\mathrm{c}}+Cu, & u\neq 0.\end{cases} \tag{10}$$

where M is the mass of the piston, L is the stroke, F_{f} is the friction force, F_{C} is the Coulomb friction force, and C is the viscous friction coefficient.

3.5 State equation

Pressure changes of the air in each chamber can be calculated by deriving the state equation of ideal gases:

$$\frac{\mathrm{d}P}{\mathrm{d}t}=\frac{1}{V}\left[\frac{PV}{\theta}\cdot\frac{\mathrm{d}\theta}{\mathrm{d}t}+R\theta G-PAu\right], \tag{11}$$

where V is the volume.

4 Dimensionless mathematical model

To facilitate the research, the assumptions made in Section 3 also apply to this section.

The reference values and the dimensionless variables are shown in Table 1. It is clear that the reference air mass flow is determined solely by the effective area of the intake and exhaust ports, the supply pressure and the temperature. The basic mathematical model can be made dimensionless as described below.

4.1 Dimensionless energy equation

The dimensionless energy equations for the discharge side and the charge side are given as

$$m^*\frac{\mathrm{d}\theta^*}{\mathrm{d}t^*}=\frac{S^*}{S_{\mathrm{b}}^*T_{\mathrm{hd}}^*}(1-\theta^*)+(k-1)(P^*u^*-G^*\theta^*), \tag{12}$$

$$m^*\frac{\mathrm{d}\theta^*}{\mathrm{d}t^*}=\left(\frac{S^*}{S_{\mathrm{b}}^*T_{\mathrm{hc}}^*}+G^*\right)(1-\theta^*)+(k-1)(G^*-P^*A^*u^*), \tag{13}$$

where the dimensionless parameter T_{hd}^* is the dimensionless temperature settling time of the discharge side, T_{hd} is the temperature settling time constant, and T_{p} is the isothermal pressure time constant (Kagawa, 1985). The dimensionless and dimensional time constants can be written as follows:

Table 1 Reference values and dimensionless variables

Variable	Reference value	Dimensionless variable
Time	$T_p=\dfrac{m_b}{G_{max}}=\dfrac{V_b}{A_eDR\sqrt{\theta_a}}$ (time to totally exhaust m_b of air at G_{max} of air mass flow)	$t^*=\dfrac{t}{T_p}$
Pressure	P_s (supply pressure)	$P^*=\dfrac{P}{P_s}$
Temperature	θ_a (atmospheric temperature)	$\theta^*=\dfrac{\theta}{\theta_a}$
Air mass flow	$G_{max}=\dfrac{A_eP_sD}{\sqrt{\theta_s}}$ (maximum air mass flow at charge side of boosting chamber)	$G^*=\dfrac{G}{G_{max}}$
Air mass	$m_b=\dfrac{P_sV_b}{R\theta_a}$ (maximum air mass in boosting chamber)	$m^*=\dfrac{m}{m_b}=\dfrac{P^*V^*}{\theta^*}$
Displacement	L (maximum displacement)	$x^*=\dfrac{x}{L}$
Volume	$V_b=L\cdot A_b$ (maximum volume of boosting chamber B)	$V^*=\dfrac{V}{V_b}$
Area of piston	A_b (area of piston in boosting chamber)	$A^*=\dfrac{A}{A_b}$

$$T_{hd}^*=\frac{T_{hd}}{T_P}, \tag{14}$$

$$T_{hd}=\frac{C_vm}{S_bh_d}, \tag{15}$$

$$S_b=2A_b+2L\sqrt{\pi A_b}. \tag{16}$$

The dimensionless maximum heat transfer area can be calculated as

$$S_b^*=\frac{2A_b+2L\sqrt{\pi A_b}}{A_b}=2+2L\sqrt{\frac{\pi}{A_b}}. \tag{17}$$

For the charge side:

$$T_{hc}^*=\frac{T_{hc}}{T_P}, \tag{18}$$

$$T_{hc}=\frac{C_vm}{S_bh_c}. \tag{19}$$

4.2 Dimensionless equation of continuity

The dimensionless equation of continuity can be given as

$$\frac{dm^*}{dt^*}=G^*. \tag{20}$$

4.3 Dimensionless flow equation

The dimensionless flow equation for both sides of the chambers becomes:

$$G^*=\begin{cases}\dfrac{P_U^*B}{D\sqrt{\theta_U^*}}\sqrt{\left(\dfrac{P_L^*}{P_U^*}\right)^{\frac{2}{\kappa}}-\left(\dfrac{P_L^*}{P_U^*}\right)^{\frac{\kappa+1}{\kappa}}}, & \dfrac{P_L^*}{P_U^*}>0.528,\\ \dfrac{P_U^*}{\sqrt{\theta_U^*}}, & \dfrac{P_L^*}{P_U^*}\le 0.528.\end{cases} \tag{21}$$

The average outlet flow of the booster can be given as

$$\overline{G}^*=\frac{m^*}{t^*}. \tag{22}$$

4.4 Dimensionless motion equation

The dimensionless equation of motion can be given as follows:

$$\frac{d^2x^*}{d(t^*)^2}=\begin{cases}(1/T_f^*)^2(P_{dA}^*A_d^*-P_{dB}^*A_d^*+P_{bA}^*-P_{bB}^*-F_f^*), & x\ne 0,1,\\ 0, & x^*=0,1,\end{cases} \tag{23}$$

where F_f^* is the dimensionless friction force, and can be written as

$$F_{\mathrm{f}}^{*}=\begin{cases}F_{\mathrm{s}}^{*}, & u=0,\\ F_{\mathrm{c}}^{*}+C^{*}u^{*}, & u\neq 0,\end{cases} \tag{24}$$

where F_{s}^{*} is the dimensionless maximum static friction force, F_{c}^{*} is the dimensionless Coulomb friction force, and C^{*} is the dimensional viscous friction force coefficient. All dimensional parameters can be written as follows:

$$F_{\mathrm{s}}^{*}=\frac{F_{\mathrm{s}}}{P_{\mathrm{s}}A_{\mathrm{b}}}, \tag{25}$$

$$F_{\mathrm{c}}^{*}=\frac{F_{\mathrm{c}}}{P_{\mathrm{s}}A_{\mathrm{b}}}, \tag{26}$$

$$C^{*}=\frac{C\cdot u_{0}}{P_{\mathrm{s}}A_{\mathrm{b}}}. \tag{27}$$

The dimensionless parameter, T_{f}^{*}, is defined in Eq. (28). T_{f}^{*} corresponds to the *J*-parameter that is used in the current selection method of a pneumatic cylinder (Ando, 1965; Kadota, 1971). The *J*-parameter is given by Eq. (30).

$$T_{\mathrm{f}}^{*}=\frac{T_{\mathrm{f}}}{T_{\mathrm{p}}}, \tag{28}$$

$$T_{\mathrm{f}}=\sqrt{\frac{ML}{A_{\mathrm{b}}P_{\mathrm{s}}}}, \tag{29}$$

$$J=\frac{T_{\mathrm{p}}^{2}P_{\mathrm{s}}A_{\mathrm{b}}}{LM}. \tag{30}$$

From Eqs. (28)–(30), the relation between T_{f}^{*} and the *J*-parameter is

$$J=\left(\frac{1}{T_{\mathrm{f}}^{*}}\right)^{2}. \tag{31}$$

Because the *J*-parameter appears as a coefficient of acceleration, it is known as the inertia coefficient, and T_{f}^{*} represents the dimensionless natural period of the booster (Tokashiki, 1999).

4.5 Dimensionless state equation

The dimensionless state equation for the discharge side and charge side becomes:

$$\frac{\mathrm{d}P^{*}}{\mathrm{d}t^{*}}=\frac{P^{*}}{\theta^{*}}\frac{\mathrm{d}\theta^{*}}{\mathrm{d}t^{*}}+\frac{\theta^{*}G^{*}}{V^{*}}-\frac{P^{*}A^{*}u^{*}}{V^{*}}. \tag{32}$$

5 Simulation study and experimental verification

5.1 Simulation study of the booster

From the discussion above, it can be found that the dimensionless outlet flow of the booster is determined by nine dimensionless parameters as above mentioned. The initial values of the nine dimensionless parameters are shown in Table 2. The software, MATLAB/Simulink, is used for modeling the simulation. The flow diagram for the solution algorithm can be seen in Fig. 3, and Fig. 4 depicts the motion characteristics of the piston and the outlet flow characteristics of boosting chamber A.

Table 2 Initial values of the dimensionless parameters

Parameter	Value	Parameter	Value
P_{r}^{*}	0.55	C^{*}	0.0008
$P_{\text{o-condition}}^{*}$	1.33	T_{f}^{*}	0.0167
A_{d}^{*}	1	T_{hc}^{*}	4.47
F_{s}^{*}	0.008	T_{hd}^{*}	2.98
S_{b}^{*}	1		

Fig. 4 shows that when the piston began to move towards the left with the increase of the pressure in boosting chamber A, the velocity of the piston dropped from the peak. When the pressure of the air in boosting chamber A was higher than the pressure of the second side, the air in boosting chamber A became exhausted, and the pressure of the air in boosting chamber A remained constant. The velocity of the piston increased and later remained steady. When the piston reached the left terminal, the air in the former working driving chamber flew to atmosphere quickly, so the pressure of boosting chamber A decreased sharply and reached the bottom. Then, the piston started to move toward the right side, and the boosting chamber A began to charge air. After a fluctuation in the pressure of boosting chamber A, the velocity of the piston and the input flow of boosting chamber A remained stable until the piston reached the right terminal.

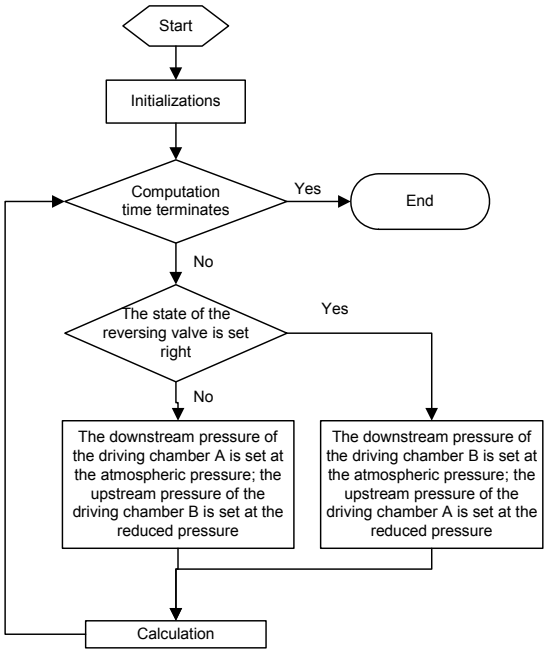

Fig. 3 Flow diagram for the solution algorithm

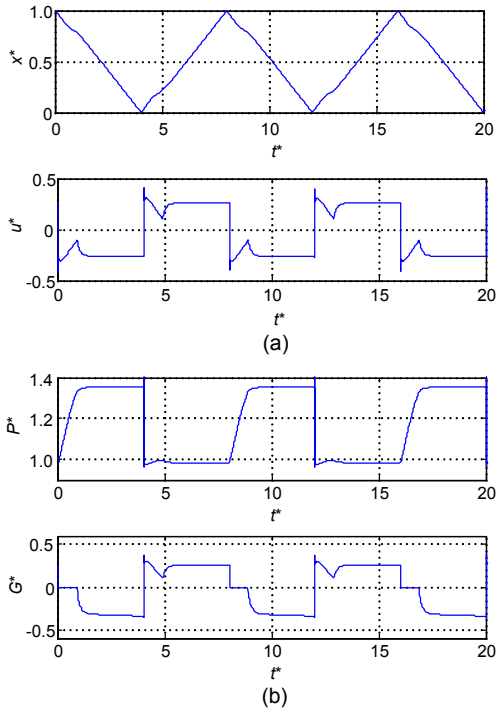

Fig. 4 Motion characteristics of the piston (a) and outlet pressure and flow of boosting chamber A (b)

5.2 Experimental verification of the mathematical model

The dimensionless outlet flow and dimensionless cycle time can be attained easily and expediently. These parameters were studied experimentally to verify the dimensionless mathematical model that was set up above.

The experimental apparatus shown in Fig. 5 consists of a booster (VBA4200), a throttle valve (AS3001F), a regulator (IR3020-03BC) by SMC, an air power meter (APM-450) by Tokyo Meter and a data acquisition card (USB-4711A) by Advantech. The air power meter adopted can simultaneously measure the pressure, flow and temperature of compressed air. The accuracy of pressure, flow and temperature is 0.1%, ±1% F.S. and 0.1 °C, respectively (Cai *et al*., 2003; 2006).

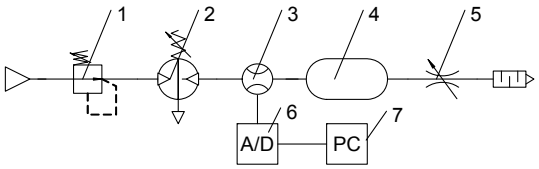

Fig. 5 Configuration of experimental apparatus
1: regulator; 2: booster; 3: air power meter; 4: tank; 5: throttle valve; 6: data acquisition card; 7: computer

In this experiment, firstly, the compressed air source was opened and the outlet pressure of the regulator was set to the fixed value. Next, adjust throttle valve and make sure that air was exhausted steadily from the tank. After that, the pressure of the air was approximately the fixed value. The last stage was data acquisition and preservation.

The experiment can be performed according to the method described above. A small outlet flow of the booster must be set so that the influence of pressure fluctuation on the supply and the tank can be reduced. The outlet flow of the booster, which was obtained by simulation and experimentation, is shown in Fig. 6.

The outlet condition pressure of the booster in the experiment study is the pressure of the compressed air in the tank. However, the outlet condition pressure of the booster in the simulation study is a constant value. The curves of the dimensionless outlet condition pressures are shown in Fig. 7.

As shown in Fig. 6 it is clear that the simulation results are consistent with the experimental results, and this verifies the mathematical model above. However, there are two differences between the simulation results and the experimental results: (1)

Outlet flow in the experiment results increases more drastically, but drops less dramatically than that in the simulation results. (2) The interval of exporting-air in the experiment is shorter than that of simulation.

The main reasons for the differences are summarized as follows. Because of persistent discharge of air from the tank, when the booster starts to exhaust compressed air, the pressure of air in the tank is the lowest, as shown in Fig. 7, the velocity of the piston increases swiftly, and the higher-pressure air in the boosting chamber is exhausted rapidly. With each additional increment of flow of air exported, the pressure of the air in the tank increases, the speed of piston decelerates, and the flow of air discharged from the booster decreases. However, the simulation is based on the assumption that the dimensionless outlet condition pressure is constant. Therefore, the experiment outlet flow rises sharply and drops slowly.

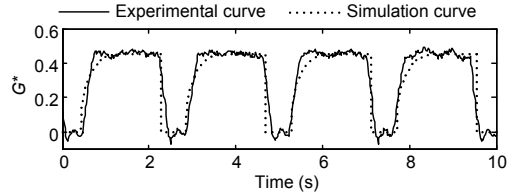

Fig. 6 Experimental and simulation curves of outlet flow of boosters

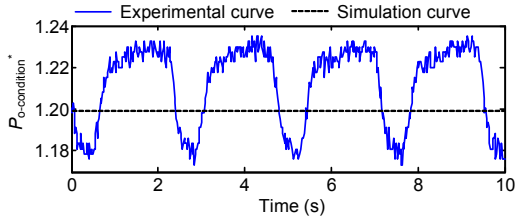

Fig. 7 Experimental and simulation curves of the dimensionless outlet condition pressure

When the booster stops to discharge compressed air, the pressure of the air in the tank starts to decrease, which is lower than the pressure of the air set in the experiment. Therefore, the booster may start to discharge air, even though the pressure of the air does not reach the pressure set, and that shortens the interval of the exporting air.

Other uncontrollable factors in the experiment, such as fluctuation of the supply pressure, leakage between chambers and temperature of the atmosphere, are also reasons for these differences between the simulation and experimental results.

6 Outlet flow characteristics

The rate of change of the dimensionless outlet flow is the ratio of the change in the outlet flow for one parameter and the total change in the outlet flow for all parameters, which is defined for evaluation of the influence of each parameter.

According to the dimensionless mathematical model above, each parameter can be changed for comparison while all other parameters are kept constant, as shown in Table 2, and the simulation results of each dimensionless parameter are illustrated in Fig. 8. Fig. 9 describes the rate of change of the outlet flow for each parameter.

It can be seen from Figs. 8 and 9 that:

1. The dimensionless outlet flow characteristic is impacted significantly by the dimensionless input pressure of the driving chambers, the dimensionless outlet condition pressure and the dimensionless area of the piston in the driving chambers. The rates of change of the outlet flow for the three parameters are 0.48, 0.26, and 0.24, respectively.

2. Especially, when the dimensionless input pressure of the driving chambers rises from 0.55 to 0.8, the dimensionless outlet flow increases from 0.24 to 0.46. When the dimensionless outlet condition pressure rises from 1.17 to 1.33, the dimensionless outlet flow decreases from 0.44 to 0.24. When the dimensionless area of the piston in the driving chambers rises from 1 to 1.5, the dimensionless outlet flow increases from 0.24 to 0.32.

3. The dimensionless outlet flow is slightly affected by the dimensionless maximum heat transfer area and the dimensionless temperature settling time of the discharge side. The rates of change of the outlet flow for the two parameters are about 0.008.

4. There is little influence of the dimensionless temperature settling time of the charge side, the dimensionless maximum static friction force, the dimensionless viscous friction force coefficient and the dimensionless natural period on the dimensionless outlet flow. The rates of change of the outlet flow for the four parameters are smaller than 0.004.

In summary, the dimensionless outlet flow of a booster is mainly determined by the dimensionless input pressure of the driving chambers, the dimensionless outlet condition pressure of the booster and the dimensionless area of the piston in the driving

chamber. The influences of the other parameters can be neglected. The conclusion agrees well with Tokashiki (1999).

The parametric study on the relationship between the dimensionless average outlet flow and the dimensionless input pressure of the driving chambers, the dimensionless outlet condition pressure, and the dimensionless area of piston in the driving chamber were conducted, and results are shown in Fig. 10.

From Fig. 10, it can be seen that the dimensionless average outlet flow increases continuously for the most part with an increase in the dimensionless

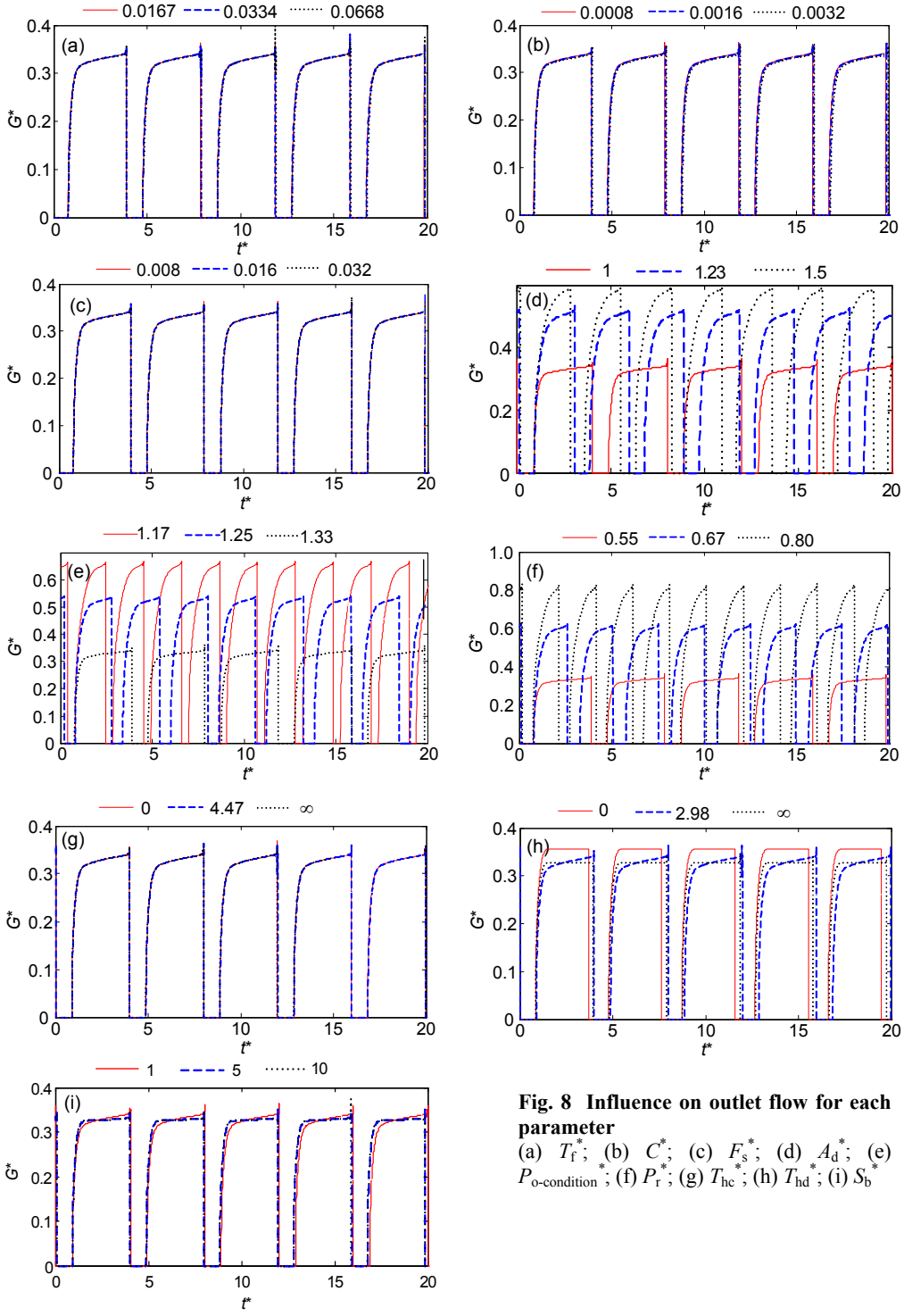

Fig. 8 Influence on outlet flow for each parameter

(a) T_f^*; (b) C^*; (c) F_s^*; (d) A_d^*; (e) $P_{o\text{-}condition}^*$; (f) P_r^*; (g) T_{hc}^*; (h) T_{hd}^*; (i) S_b^*

input pressure of the driving chambers; however, the dimensionless average outlet flow decreases non-linearly with an increase in the dimensionless outlet condition pressure, and the dimensionless average outlet flow reaches zero when the dimensionless outlet condition pressure is approximately 1.4. At the beginning, the dimensionless average outlet flow increases with increasing dimensionless area of the piston in the driving chamber and peaks at approximately 1.89. After this peak, the dimensionless average outlet flow starts to decrease with increasing dimensionless area of the piston in the driving chamber.

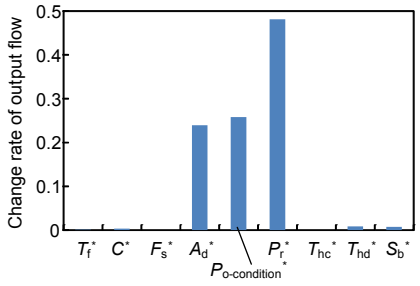

Fig. 9 Rate of change of outlet flow for each parameter

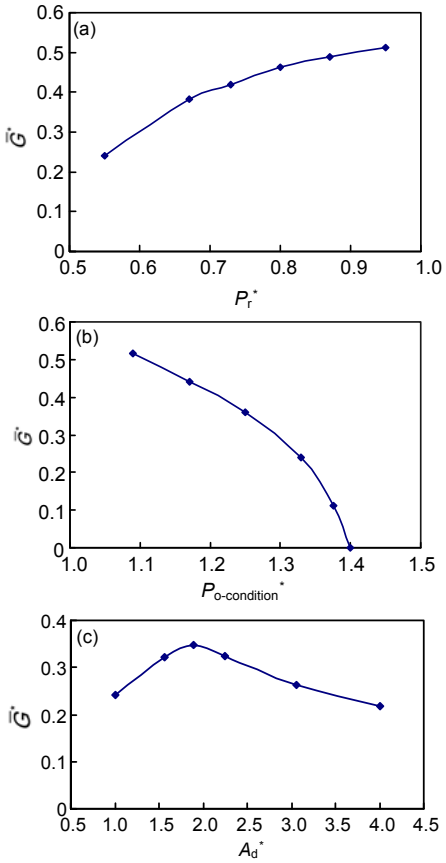

Fig. 10 Outlet flow characteristics of the booster
(a) Relationship between outlet flow and P_r^*; (b) Relationship between outlet flow and $P_{o\text{-}condition}^*$; (c) Relationship between outlet flow and A_d^*

7 Conclusions

The boosting process of an air-driven booster was studied, and a basic mathematical model was developed. Appropriate reference values were selected, the basic mathematical model was transferred to a dimensionless expression, and the outlet flow was analyzed through simulation and experimentation. The conclusions can be drawn as follows:

1. Simulation results agree well with experimental results, and the mathematical model set above is correct.

2. The outlet flow characteristics of the booster are mainly determined by the dimensionless input pressure of the driving chambers, the dimensionless outlet condition pressure of the booster, and the dimensionless area of the piston in the driving chamber. The influence of all other parameters can be neglected.

The dimensionless average outlet flow increases steadily for the most part, with increasing dimensionless input pressure of driving chambers, but it decreases non-linearly with increasing dimensionless outlet condition pressure. When the dimensionless outlet condition pressure is approximately 1.4, the dimensionless average outlet flow reaches zero. At the beginning, the dimensionless average outlet flow increases with increasing dimensionless area of the piston in the driving chamber and peaks at approximately 1.89. Next, the dimensionless average outlet flow starts to decrease with increasing dimensionless area of the piston in the driving chamber.

References

Ando, K., 1965. Study on Characteristics of Pneumatic Systems for Resistance Welding Machines. The Japan Welding Engineering Society, Tokyo, Japan (in Japanese).

Cai, M.L., Funaki, T., Kawashima, K., Kagawa, T., 2003. Development of Pneumatic Power Meter for Energy Saving. Proceedings of Symposium on Fluid Power System at Spring, Tokyo, Japan, p.119-121.

Cai, M.L., Kawashima, K., Kagawa, T., 2006. Power assessment of flowing compressed air. *Journal of Fluids Engineering, Transactions of the ASME*, **128**(2):402-405. [doi:10.1115/1.2170129]

Chapman, K.S., Keshavar, A., Wolfram, K., 2008. Increasing Turbocharged Engine Operating Ranges through Use of a Booster System. Proceedings of the Fall Technical Conference of the ASME Internal Combustion Engine Division, Charleston, USA, p.473-480. [doi:10.1115/ICEF2007-1806]

Cheng, H.P., Chen, C.J., Cheng, P.W., 2003. Computational fluid dynamics performance estimation of turbo booster vacuum pump. *Journal of Fluids Engineering*, **125**(3): 586-589. [doi:10.1115/1.1566042]

Cho, N.C., Hwang, I.J., Lee, C.M., Park, J.W., 2009. An experimental study on the airlift pump with air jet nozzle and booster pump. *Journal of Environmental Sciences*, **21**(Suppl.1):S19-S23. [doi:10.1016/S1001-0742(09)60028-0]

Ge, Y.T., Tassou, S.A., 2011. Thermodynamic analysis of transcritical CO_2 booster refrigeration systems in supermarket. *Energy Conversion and Management*, **52**(4): 1868-1875. [doi:10.1016/j.enconman.2010.11.015]

Hernández, J.I., 2005. Study of a solar booster assisted ejector refrigeration system with R134a. *Journal of Solar Energy Engineering, Transactions of the ASME*, **127**(1):53-59. [doi:10.1115/1.1771683]

Kadota, U., 1971. Characteristics of air (13). *Hydraulics and Pneumatics Design*, **9**(2):109-115.

Kagawa, T., 1985. Heat transfer effects on the frequency response of a pneumatic nozzle flapper. *Journal of Dynamic Systems, Measurement and Control*, **107**(4): 332-336.

Li, Z.Y., Zhao, Y.Y., Li, L.S., Shu, P.C., 2007. Mathematical modeling of compression processes in air-driven boosters. *Applied Thermal Engineering*, **27**(8-9):1516-1521. [doi:10.1016/j.applthermaleng.2006.09.012]

Reed Business Information (Cahners), 2003. Pressure boosters allow natural gas to do more. *Plant Engineering (Barrington, Illinois)*, **57**(12):A4-A5.

Shi, Y., Cai, M.L., 2011. Working characteristics of two kinds of air-driven boosters. *Energy Conversion and Management*, **52**(12):3399-3407. [doi:10.1016/j.enconman.2011.07.008]

Shi, Y., Cai, M.L., Liao, P.P., 2010a. Flow characteristics of pneumatic booster regulator. *Journal of Harbin Institute of Technology*, **42**(12):2013-2016 (in Chinese).

Shi, Y., Cai, M.L., Wang, G.P., 2010b. Study on air-supplied with different pressure and locally pressure-boosting technology of pneumatic system. *Machine Tool & Hydraulics*, **38**(9):57-59 (in Chinese).

SMC (China) Co., Ltd, 2008. Modern Practical Pneumatic Technology, 3rd Edition. Machine Press, Beijing, China, p.310-316 (in Chinese).

Takeuchi, O., Fujita, T., Kagawa, T., 1995. Characteristics Analysis of Expanding-Type Booster. Proceedings of Autumn Symposium on Hydraulics and Pneumatics, Tokyo, Japan, p.69-72 (in Japanese).

Tokashiki, K., 1999. Dynamic Characteristics of Pneumatic Cylinder Systems. Department of Control Engineering, Tokyo Institute of Technology, Tokyo, Japan.